ELSEVIER

Journal of Chromatography B, 740 (2000) 17–33

JOURNAL OF CHROMATOGRAPHY B

www.elsevier.com/locate/chromb

New strategy for the design of ligands for the purification of pharmaceutical proteins by affinity chromatography

Kenny Sproule[a], Paul Morrill[a], James C. Pearson[b], Steven J. Burton[b], Kim R. Hejnæs[c], Henrik Valore[c], Svend Ludvigsen[c], Christopher R. Lowe[a,*]

[a]*Institute of Biotechnology, University of Cambridge, Tennis Court Road, Cambridge CB2 1QT, UK*
[b]*ProMetic BioSciences Inc., 307 Huntingdon Road, Girton, Cambridge CB3 OJX, UK*
[c]*Novo Nordisk A/S, Novo Allé, DK-2880 Bagsværd, Denmark*

Received 13 August 1999; received in revised form 18 November 1999; accepted 17 December 1999

Abstract

A new approach for the identification of ligands for the purification of pharmaceutical proteins by affinity chromatography is described. The technique involves four steps. Selection of an appropriate site on the target protein, design of a complementary ligand compatible with the three-dimensional structure of the site, construction of a limited solid-phase combinatorial library of near-neighbour ligands and solution synthesis of the hit ligand, immobilisation, optimisation and application of the adsorbent for the purification of the target protein. This strategy is exemplified by the purification of a recombinant human insulin precursor (MI3) from a crude fermentation broth of *Saccharomyces cerevisiae*.

Keywords: Chemical combinatorial library; Proteins; Ligands; Insulin

1. Introduction

The ability to produce substantial quantities of pure, safe and efficaceous therapeutic protein from isolated genes is an on-going challenge for the biotechnology industry. The impact of human genomics, together with cost-containment in healthcare management, environmental and safety legislation, and the imminent appearance of generic biopharmaceuticals, is likely to drive the industry towards the introduction of high throughput, cost-effective and flexible manufacturing processes based on new technology. Highly selective techniques such as affinity chromatography are expected to play an increasing role in bioprocessing, since, not only do they satisfy the requirement for the ultra-high resolution of the target protein from other inert and host proteins present in the expression system, but they also remove bioactive contaminants such as DNA, glycolipids, toxins and viruses, and structural isoforms of the target protein itself, thereby providing in-built quality assurance [1]. Unfortunately, many of the current affinity adsorbents based on natural biological ligands such as proteins and peptides are fragile, expensive and not readily amenable to scale-up and ruggedisation for the harsh manufacturing environment of the biopharmaceutical industry. For example, while adsorbents based on monoclonal

*Corresponding author. Tel.: +44-1223-334-160; fax: +44-1223-334-162.
E-mail address: crl1@biotech.cam.ac.uk (C.R. Lowe)

0378-4347/00/$ – see front matter
PII: S0378-4347(99)00570-8

antibodies [2], phage display peptides [3] or mimotopes [4] are superficially attractive, they may suffer from problems associated with reduced capacity when the ligand is immobilised, toxic or bioactive leachates, retroviral contamination and an inability to be sterilised or cleaned-in-place. Thus, in order to create high capacity adsorbents capable of withstanding the rigours of depyrogenation, sterilisation and cleaning-in-place during multiple operational cycles, while retaining their ability to adsorb and elute native proteins in high yield, careful consideration must be given to the design of the complete adsorbent, including the matrix, activation and coupling chemistry, spacer molecule and, in particular, the biospecific ligand. Early work on ''biomimetic'' ligands, based initially on textile dyes [5,6] and subsequently on ligands designed to mimic natural motifs such as dipeptides [7,8], provided proof of concept. A synthetic bis-substituted triazine ligand devoid of fissile bonds was designed and synthesised as an analogue of the side chains of the natural Phe–Arg dipeptide substrate of pancreatic kallikrein, and, when immobilised to agarose, was able to resolve kallikrein from the homologous proteinase trypsin, and purify the enzyme from crude pancreatic extracts [7]. More recently, a triazine ligand selective for IgG was created by mimicking a template comprising the key Phe^{132}–Tyr^{133} dipeptide motif of the B domain of protein A, synthesised, characterised and shown to purify IgG from human plasma and ascites fluid [8]. The inherent stability of these novel ligands allowed repeated use with stringent intervening sterilisation and cleaning procedures.

The rational de novo design of affinity ligands has been restricted to date to a limited number of target proteins where a suitable template structure derived from known substrates [7] or complementary binding molecules [8] is available. A more general approach to the construction of biomimetic matrices exploits knowledge of the target protein per se, preferably in association with access to combinatorial ligand libraries [9] and effective screening protocols. In this paper, we report the implementation of a new rational design and combinatorial library strategy for ligand synthesis based exclusively on the selection of an appropriate site on the target protein, design of a complementary ligand compatible with the crystallographic structure of the site, and construction of a limited combinatorial library of near-neighbour ligands. A recombinant human insulin precursor expressed in *Saccharomyces cerevisiae* and designated MI3 was used as the target protein.

2. Experimental

2.1. Computer-aided molecular modelling

Molecular modelling, molecular design and all calculations were performed on a Silicon Graphics 4D/35 Personal Iris work station (Silicon Graphics, Reading, UK) with a Quanta 4.0 Software package (Molecular Simulations, Burlington, USA).

2.2. Solid-phase synthesis of ligand library

Amino-derivatised agarose 6XL (ProMetic BioSciences, Balasalla, Isle of Man) (24 μmol amino groups/g moist weight gel; 110 g) was gently stirred in acetone–water (1:1, v/v; 200 ml, 0°C) in an ice–salt bath and a solution of 1,3,5-trichlorotriazine (5 mmol, 0.9 g) in acetone (30 ml) added at 0°C in small portions over a period of 2 h. When amine could no longer be detected with ninhydrin, the triazine-activated agarose was washed sequentially with increasing concentrations of acetone in water, 100% acetone (4×500 ml), decreasing concentrations of acetone in water and, finally, water (4×250 ml). The activated agarose was stored in isopropanol–water (30:70, v/v, 100 ml) and used for synthesis of the ligand library within 24 h. Moist activated agarose (100 g) was divided into four equal parts (25 g) and added to a solution of the first amine (1.2 mmol, 2 equivalents) dissolved in 50% (v/v) acetone (25 ml) and agitated gently at 30°C for 16 h. The substituted gels were separately recovered on a glass sinter (No. 2) and washed exhaustively with 50% (v/v) acetone (200 ml), 80% (v/v) acetone (200 ml) and 100% acetone (200 ml) and then with decreasing concentrations of acetone from 80% (v/v) to 0% in 100-ml volumes. The filtered and washed monosubstituted agarose gels were each divided into four portions (5 g moist gel), whence, to each of the 16 gels in glass universal bottles was added a solution of 50% (v/v) dimethylforamate (DMF) (5 ml) containing the second amine substituent (0.24 mmol,

2 equivalents) and the reactions allowed to proceed with rotational agitation at 80–90°C for 72 h in an oven. A molar equivalent of NaOH was added to the reaction mixture where the amino ligand bore a carboxyl function. The bisubstituted gels were separately washed and filtered as described above and were stored in 20% (v/v) ethanol at +4°C.

2.3. Solution phase synthesis of ligands 2/2 and 23/23

Two procedures were used to synthesise these ligands in solution. In the first method, 1,3,5-trichlorotriazine (10.8 mmol, 2 g) was recrystallised from 80 to 100°C petroleum ether dissolved in acetone (60 ml), added in small portions over 30 min to a stirred ice cooled solution of 1-amino-5-naphthol (Table 1; 2) or 1-amino-7-naphthol (Table 1; 23) (24 mmol, 3.8 g) in acetone–water (80:20, v/v) (200 ml) and stirred for a further 24 h at 30°C. The HCl generated during the reaction was neutralised through periodic addition of sodium carbonate to a total of 1 equivalent. The reaction was monitored by thin-layer chromatography (TLC) (ethyl acetate–hexane, 1:4, v/v) until only bis-substituted triazine could be detected, whence the product was precipitated from the reaction mixture by the addition of 1 *M* HCl and water. In the second procedure, 1-amino-5-naphthol (Table 1; 2) or 1-amino-7-naphthol (Table 1; 23) (13.9 mmol, 2.2 g) was dissolved in dioxane (20 ml), whence half (10 ml) was added in small portions over 30 min to a stirred solution of 1,3,5-trichlorotriazine (6.28 mmol, 1.16 g) maintained at 4°C. The temperature of the reaction mixture was allowed to rise to 20°C and the remaining aminonaphthol solution added together with diisopropylethylamine (25.2 mmol, 2.16 ml). The reaction was monitored by TLC (toluene–methanol, 5:1, v/v) until only bis-substituted triazine could be detected, whence the product was precipitated from the reaction mixture by the addition of 1 *M* HCl. Both synthetic protocols generated the same products

Table 1
List of amines substituted on the triazine scaffold for the construction of the insulin analogue (MI3) binding combinatorial library

Amines	Chemical name
1	1-Amino-6-naphthalene sulphonic acid
2	1-Amino-5-naphthol
3	Benzylamine
4	3,5-Diaminobenzoic acid
5	3-Aminobenzoic acid
6	4-Aminobenzoic acid
7	Tyramine
8	Naphthylamine
9	4-Nitro-1-aminonaphthylamine
10	2,7-Diaminofluorene
11	3,6-Diaminoacridine
12	3-Amino-1,2-propanediol
13	3-Amino-1-propanol
14	5-Amino-1-pentanol
15	3-Aminophenol
16	6-Aminocaproic acid
17	3-Aminophenylboronic acid
18	3-Amino-2-naphthoic acid
19	4-Amino-1-naphthol
20	1-Amino-2-naphthol
21	3-Amino-2-naphthol
22	1-Amino-6-naphthol
23	1-Amino-7-naphthol
24	2-Amino-1-naphthol
25	6-Amino-1-naphthol
42	5-Aminoindan

in yields of approximately 80–90% and purities >95% by TLC. Purity analysis was also performed by reversed-phase high-performance liquid chromatography (HPLC) using a C_{18} column (Phase-Sep 839540, 25 cm, S5ODS2) with a gradient from mobile phase A [0.2% (w/v) cetyltrimethylammonium bromide] in water to mobile phase B (methanol) according to the regime: 0 min (50% B), 15 min (100% B), 25 min (100% B), 26 min (50% B), 30 min (50% B) at a flow-rate of 1 ml/min and 20°C. Detection was performed at 254 nm. The identities of the products were confirmed by mass spectrometry (MS) and ^{1}H-nuclear magnetic resonance (NMR).

2.4. Screening of the ligand library

Each affinity gel was packed to a 1 ml volume in 4-ml syringe columns and retained between 20 μm frits. The columns were washed with regeneration buffer (30%, v/v, isopropanol–0.2 *M* NaOH, 70 ml) until no ligand leakage was detected at 254 nm and then with water (20 ml). The columns were equilibrated (30 column volumes) with 0.2 *M* sodium acetate–0.1 *M* NaCl, pH 5.0 buffer at room temperature and a sample (600 μg MI3/g moist weight gel) of centrifuged and pH-adjusted (pH 5.0, solid Tris) fermentation broth containing MI3 insulin precursor applied. The columns were washed with equilibration buffer (12 ml) followed by elution with 2 *M* acetic acid (3 ml). The sample, flow through and elution fractions collected for each column were analysed for MI3 by reversed-phase HPLC. Columns were rejuvenated by washing with regeneration buffer (30 ml) and stored in ethanol–water (20:80, v/v).

2.5. Determination of the association equilibrium constants

Each of the immobilised affinity ligands were dried on a No. 3 sinter funnel, whence an aliquot (0.2 g) was weighed, rehydrated (≈0.325 ml wet volume gel) in deionised water and packed in a Pharmacia HR 5/2 column. The columns were equilibrated with a 0.1 *M* sodium acetate buffer, pH 4.5 on a BioCad 700E Workstation prior to evaluation. Purified MI3 (0–4 mg/ml; 15 ml) was applied through a 15-ml sample loop at a flow-rate of 0.3 ml/min, whence an elution/regeneration buffer comprising 30% (v/v) isopropanol–0.2 *M* NaOH (15 ml) was applied at 0.3 ml/min and the column re-equilibrated with the acetate buffer. The frontal chromatograms were monitored with a UV detector set at 280 nm. From the breakthrough curves generated at each MI3 concentration in triplicate, 50% of the optical density at steady state was used to determine the elution volume of MI3 (V_A). The column bed volume (V'_A) was determined by using the same gel volume of unmodified matrix and determining the breakthrough curve of MI3 at 2.0 mg/ml. The data were analyzed according to Winzor [10,11].

2.6. Affinity chromatography

Centrifuged fermentation broth adjusted to pH 5.5 with acetic acid and containing 0.1 *M* NaCl was applied to a column (16×25 mm XK16, Pharmacia Biotech, Sweden, 5.0 ml) packed with the appropriate 2/2 or 23/23 affinity matrix at ambient temperature using either a BioCad (Perseptive Biosystems) or Äkta (Pharmacia Biotech, Sweden) chromatography system. The optical density was recorded at 280 nm (3 mm path length). The columns were washed with 0.2 *M* and 0.1 *M* sodium acetate, pH 5.5, whence the MI3 was eluted in 0.3 *M* acetic acid at a linear flow-rate of 30 cm/h. Columns were cleaned-in-place in 0.5 *M* NaOH followed by 0.1 *M* citric acid–60% (v/v) ethanol and re-equilibrated in 0.2 *M* sodium acetate, pH 5.5.

2.7. Reversed-phase HPLC

Samples (100 μl) containing 10–25 μg protein were diluted in 2 *M* acetic acid prior to application to a C_{18} YMC 120 Å, 5 μm OdDMeSi B564 column (250×4.0 mm) using a Waters HPLC system comprising a 510 pump, 710B wisp injector, Model 440 detector (214 nm) and ExpertEase Chromatography Software, version 3.0. The chromatogram was developed over a total run time of 35 min by binary gradient elution from 36% (v/v) buffer A [0.2 *M* Na_2SO_4, 0.04 *M* H_3PO_4, 10% (w/v) CH_3CN, pH 2.3] to 60% (v/v) buffer B [50% (v/v) CH_3CN] over

20 min at 1.0 ml/min and 50°C. Detection was achieved at 214 nm with a 10 mm pathlength cell.

2.8. Sodium dodecyl sulphate gel electrophoresis

Samples were heated at 70°C for 10 min in sodium dodecyl sulphate (SDS) NuPAGE non-reducing sample buffer and an aliquot (1 μg) applied to a SDS NuPAGE 4–12% precast gel. Electrophoresis was effected in an Xcell II mini cell system at 200 V for 35 min. The gels were stained with Coomassie brilliant blue R-250 or silver.

2.9. NMR spectroscopy

Human insulin analogue MI3 (1 m*M*) was dissolved in $^{2}H_{2}O$–water containing 0.1 *M* deuterated sodium acetate, pH 4.74 (10:90, v/v). Ligand 23/23 was dissolved in d^{6}-dimethyl sulphoxide (DMSO) and added in 1:1 and 1:2 molar ratios (MI3:ligand) as 4-μl and 8-μl aliquots, respectively to a total sample volume of 800 μl. One- and two-dimensional ^{1}H-NMR spectroscopy was conducted on a 600 MHz Varian Unity instrument. Samples were allowed to equilibrate for 2 h at 20°C prior to recording the NMR spectrum.

3. Results and discussion

3.1. The design strategy

The MI3 capture adsorbent should comply with a number of specifications in order to prove acceptable for the large-scale purification of the recombinant insulin precursor. For example, it should be able to isolate the protein at pH 3.0–9.0 directly from the fermentation broth. The adsorbent should operate at pH 2.0–11.0 and 4–25°C with a dynamic capacity in the range 5–10 mg/ml and elute MI3 at a concentration ≥2.0 mg/ml, with a purity ≥95% and a recovery ≥90%. The adsorbent itself should comprise a rigid support matrix capable of sustaining linear flow-rates of ≥100 cm/h, be able to withstand 8 *M* urea, 70% (v/v) ethanol, 0.5–1.0 *M* NaOH or steam sterilisation (121°C; 30 min) and be capable of use for >200 cycles before replacement. The affinity ligand should preferably exhibit a K_{d} of 10^{-4}–10^{-5} *M*, be non-toxic and not be directed against the tripeptide bridge between A1 and B29 (Fig. 1a), although the dimer interface region would be acceptable, and perhaps preferred, in view of its potential utility in targeting the monomeric protein.

Native human insulin is a 51-residue M_{r} 5808 globular protein comprising two polypeptide chains, an A-chain of 21 residues and a B-chain of 30 residues, with a single intrachain disulphide on the A chain and two interchain disulphide bridges [12]. In solution, insulin displays a complex pattern of aggregation and precipitation dependent on pH, ionic strength, temperature, metal ions, protein concentration and solvent composition [13]. In the millimolar concentration range in aqueous solution, dimers and higher oligomers predominate at pH 2.0–3.5. As the pH is raised, aggregation increases until precipitation occurs in the pH range 4.2–6.6; above this pH, insulin gradually dissolves into dimers and higher aggregates until the monomeric state is finally reached at pH>10. The M_{r} 5959 recombinant insulin analogue used in this study, MI3, differs from human insulin by having a truncated B chain (des-B:30-Thr) and the presence of a tripeptide Ala–Ala–Lys bridge joining the C-terminus of the B-chain (B:29) to the N-terminus of the A-chain (A:1) (Fig. 1a). The solution structure of MI3 is unknown, although it can be inferred from the structure of a mutant human insulin (B:16-Tyr→His) [14] by substituting B:16-His to the wildtype residue Tyr and constructing the MI3 tripeptide bridge between B:29 and A:1. The MI3 structure [15], like other crosslinked insulins and the B:16-Tyr→His mutant [14] have structures similar to human insulin and readily form dimers and hexamers. The precise configuration of the tripeptide crosslink is less relevant to this study. Examination of this reconstructed MI3 structure revealed that the total solvent accessible surface (494 $Å^{2}$) of the protein comprised a relatively high proportion of hydrophobic (205 $Å^{2}$) and neutral polar amino acid residues (289 $Å^{2}$) but contained no obvious grooves or pockets into which the affinity ligand could be directed (Fig. 1b) [15]. However, a characteristic feature of the protein was a substantial hydrophobic area comprising several aromatic residues which constitutes the site at which dimerisation occurs [13]. This interface contains the aromatic side chains of three tyrosine residues (B:16-Tyr; A:19-Tyr; B:26-

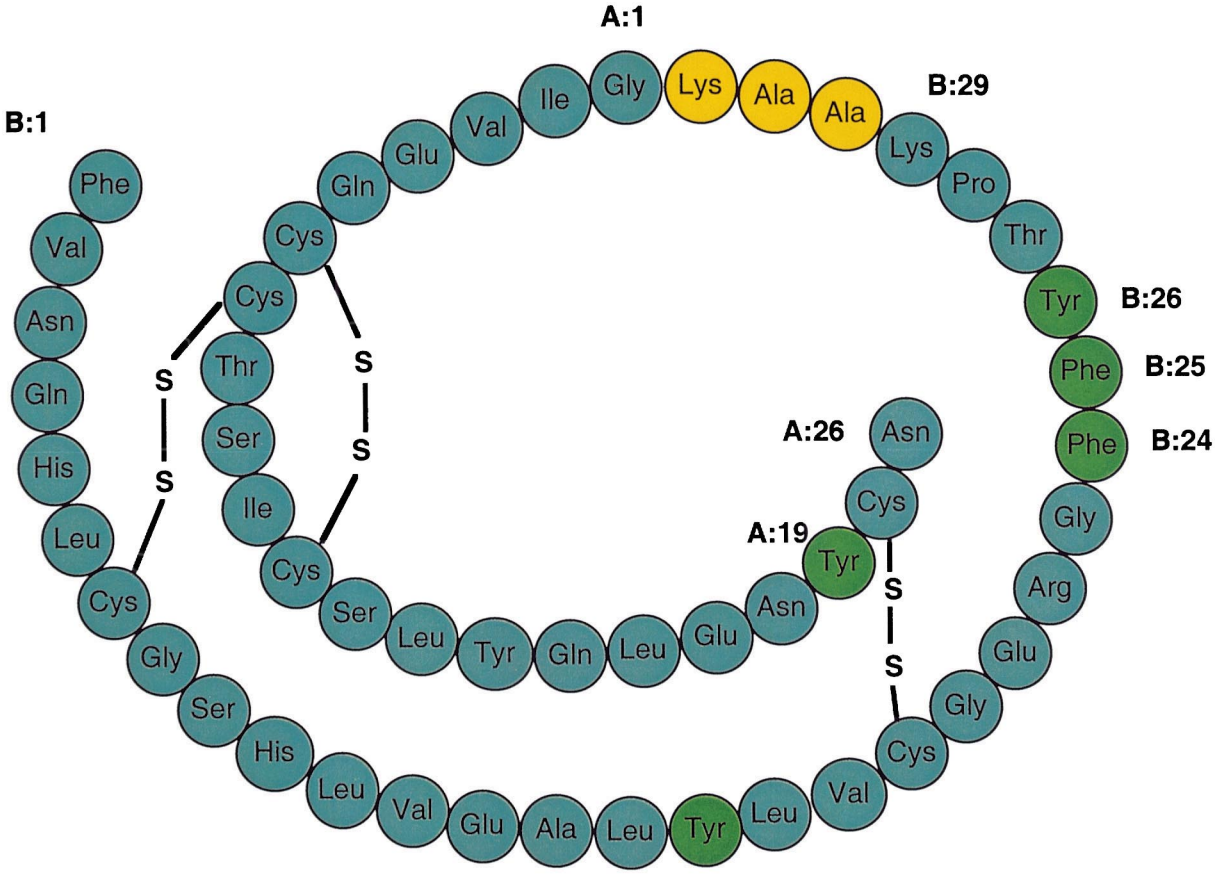

Fig. 1. The structure of the human insulin analogue MI3 showing (a) the amino acid sequence with the tripeptide bridge joining the N-terminus of the A chain (A:1) to the C-terminus of the B chain (B:29) and the three disulphide bonds, (b) the modelled structure highlighting the key aromatic residues in green forming the dimer binding interface, and (c) the putative lead compound in yellow shown interacting with two residues, B:16-Tyr and B:24-Phe.

Tyr) and two adjacent phenylalanine residues (B:24-Phe; B:25-Phe) and forms a broad swathe across the waist of the globular protein (Fig. 1b). Residues B:16-Tyr and B:24-Phe are relatively accessible to solvent, 72% and 19% of the total surface area of the residue, respectively, while B:25-Phe appears to be in an exceptionally exposed environment (77% solvent accessible surface). The presence of these aromatic residues prompted the suggestion that a suitably designed affinity ligand could bind to this region through aromatic stacking interactions [7,8].

Inspection of the dimer binding interface in more detail revealed that the side chains of two of the aromatic residues in this region, B:16-Tyr and B:24-Phe, appeared to have an orientation not unlike that of the Phe^{132}–Tyr^{133} dipeptide motif of the B-domain of protein A and used previously for the design of a highly effective ligand specific for human IgG [8]. Preliminary computer-aided molecular modelling showed that this ligand, based on a triazine scaffold substituted with aniline and tyramine, showed significant π–π overlap with the aromatic side chains of B:16-Tyr and B:24-Phe (Fig. 1c) and was thus used to indicate the type of ligand that might be used

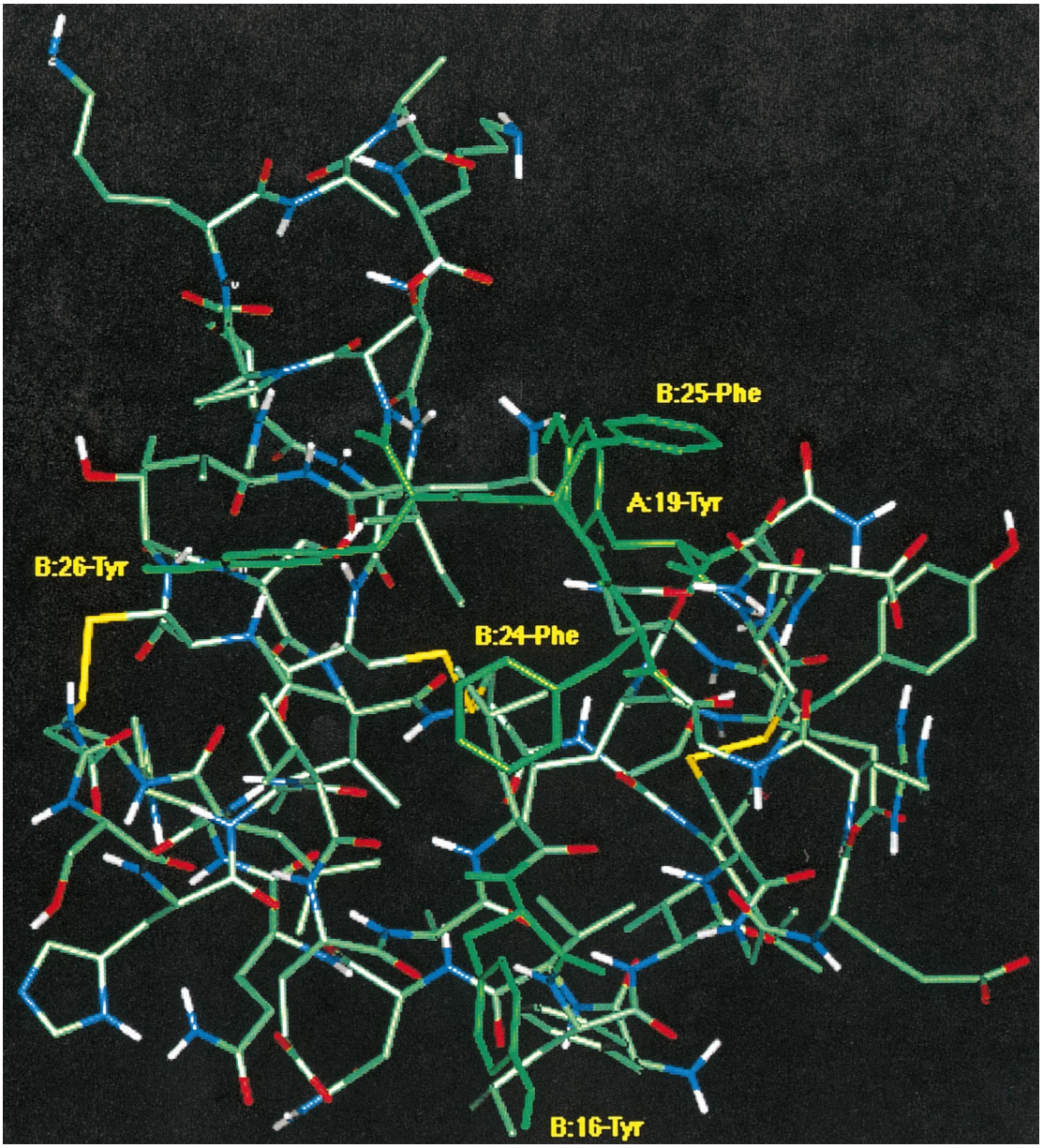

Fig. 1 (*continued*).

to construct a small combinatorial library of near-neighbour structures which retained the aromatic character of the original lead. However, it should be noted that while the B:16-Tyr/B:24-Phe diad was selected as the putative target, other adjacent aromatic residues were considered binding targets with equal potential and amenability to probing with the same directed combinatorial library.

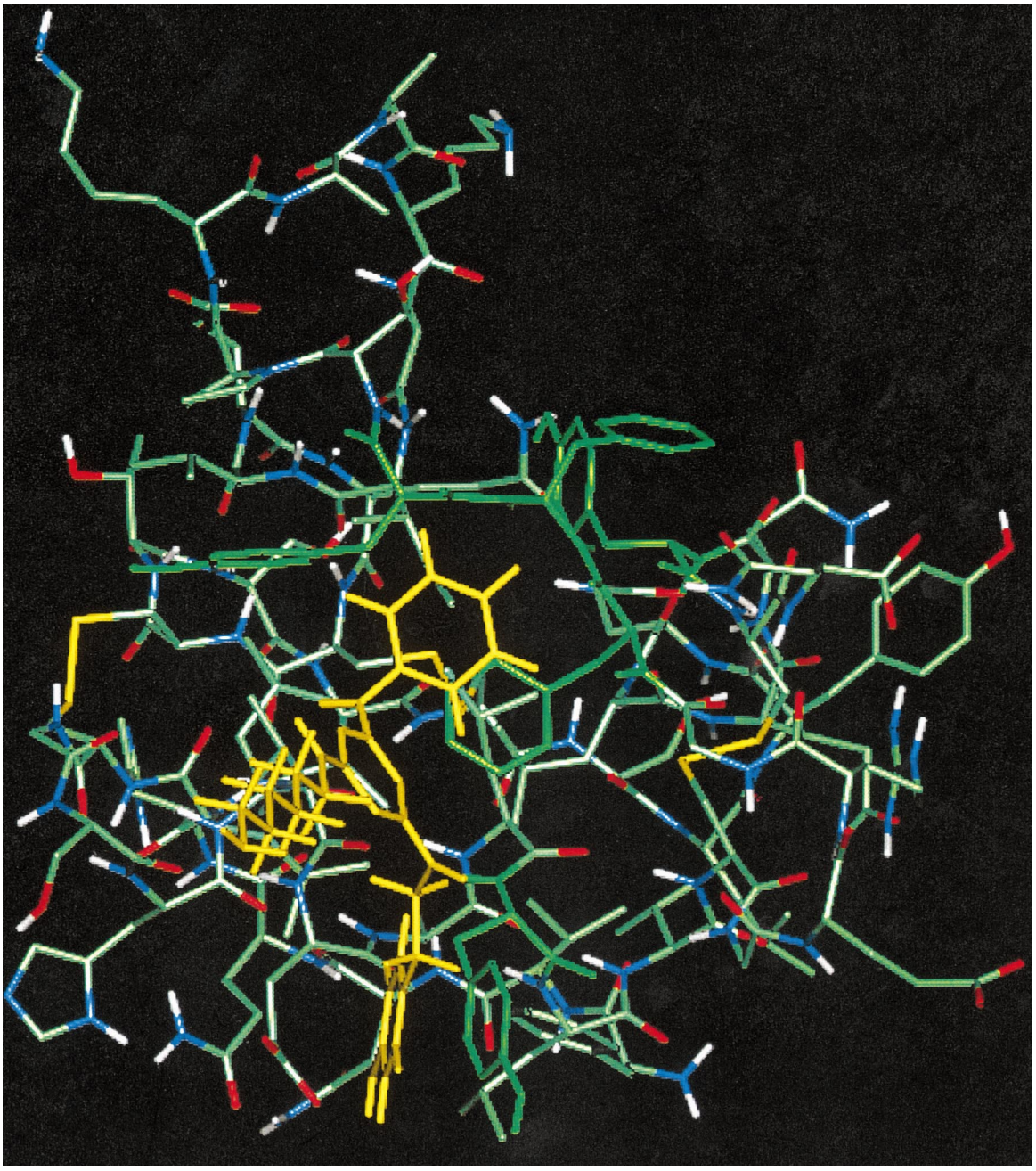

Fig. 1 (*continued*).

3.2. Construction of the rational combinatorial library

A collection of 26 amino derivatives of bi-, tri- and heterocyclic aromatics, aliphatic alcohols, fluorenes and acridines substituted with various hydroxyl, nitro, sulphonate and carboxyl functionalities formed the basis of the limited combinatorial library (Table 1). The synthesis of the ligand library was expedited by execution of a solid-phase protocol directly on chromatographic grade cross-linked agarose beads. Solution phase chemistries have been well characterised for the substitution of amines onto 1,3,5-*sym*-trichlorotriazine or cyanuric chloride [16]. In general, the three chlorine atoms can be sequentially displaced in a controlled fashion by amines in aqueous solution at approximately 0, 30–50 and 70–100°C, respectively [17]. The solid-phase library was constructed by immobilising cyanuric chloride at 0°C onto amino-agarose (24 μmol amino groups/g moist weight gel) and sequential substitution of the immobilised dichlorotriazine with either an excess, or a two-fold molar excess of the selected amines at 30°C for 24 h and subsequently a five-fold molar excess at 95°C for 72 h. This solid-phase route was well suited to the defined synthesis of small groups of similar ligands directly on agarose beads and was implemented in a discovery cycle as part of the design protocol. A library of 64 affinity ligands based on the triazine scaffold was generated in the course of this discovery process out of a potential maximum of 338 with the 26 different amines selected.

3.3. Screening of the combinatorial library for MI3 binding and elution

The pH of clarified fermentation broth containing MI3 was adjusted to 5.0 with solid Tris and a sample (600 μg MI3/g moist weight gel) applied to each member of the agarose-immobilised ligand library equilibrated with 0.2 *M* sodium acetate–0.1 *M* NaCl, pH 5.0. Samples of the void, wash and elution fractions from each column were analyzed by reversed-phase HPLC by reference to the known elution behaviour of authentic MI3.

The screening results for the chromatographic recovery of MI3 from crude fermentation broth for the entire library of ligands are shown in Fig. 2. Analysis of the adsorption and elution characteristics of MI3 on the 64-member library of immobilised ligands revealed a marked diversity in chromatographic behaviour among individual adsorbents of the library, despite similarities in structure of the triazine ligands. Under the designated conditions, the recovery of MI3 typically fell into three broad ranges: ~10%, 40–60% and 70–100%. Interestingly, the ligand designed originally to bind human IgG and modelled on a dipeptide motif of protein A [8], which was used as the starting point for the combinatorial library, displayed no affinity for purified MI3. The most effective ligands appeared to be symmetrical triazines bis-substituted with amino-naphthols or amino-naphthoic acid, such as 1-amino-5-naphthol (Fig. 3a; ligand 2/2), 3-amino-2-naphthoic acid (Fig. 3b; ligand 18/18), 1-amino-7-naphthol (Fig. 3c; 23/23) and 6-amino-1-naphthol (Fig. 3d; ligand 25/25). Under the conditions selected for the initial screen of the library, typical recoveries of MI3 from the crude broth with these adsorbents were ~60–85%.

Closer examination of the effect of the structure of the ligand on MI3 binding revealed a high degree of selectivity for MI3; for example, those ligands comprising 1-amino-naphthalene bearing hydroxylic functions in positions 5, 6 or 7 of the bicyclic nucleus proved very effective adsorbents with recoveries of MI3 typically in the 60–85% range, while those ligands bearing hydroxylic substituents at positions 2 and 4 proved very poor adsorbents, with MI3 recoveries ~10%. A similar pattern was observed with hydroxylic isomers in the 2-amino-naphthol series. Modelling studies have shown that bi-symmetrical ligands such as 23/23 (Fig. 3c) display more complete π–π overlap with the side chain aromatic rings of residues B:16-Tyr and B:24-Phe (Fig. 3e) than the single aromatic ring substituents of the original lead compound used to guide the synthesis of the directed library (Fig. 1c). However, despite the value of computer modelling to visualise putative interactions between the ligand and the dimer binding interface of the MI3, it is important to realise that the formation of intramolecular bonds within the ligand, and intermolecular interactions with other adjacent ligands, the coupling and spacer chemistries and the matrix backbone, also

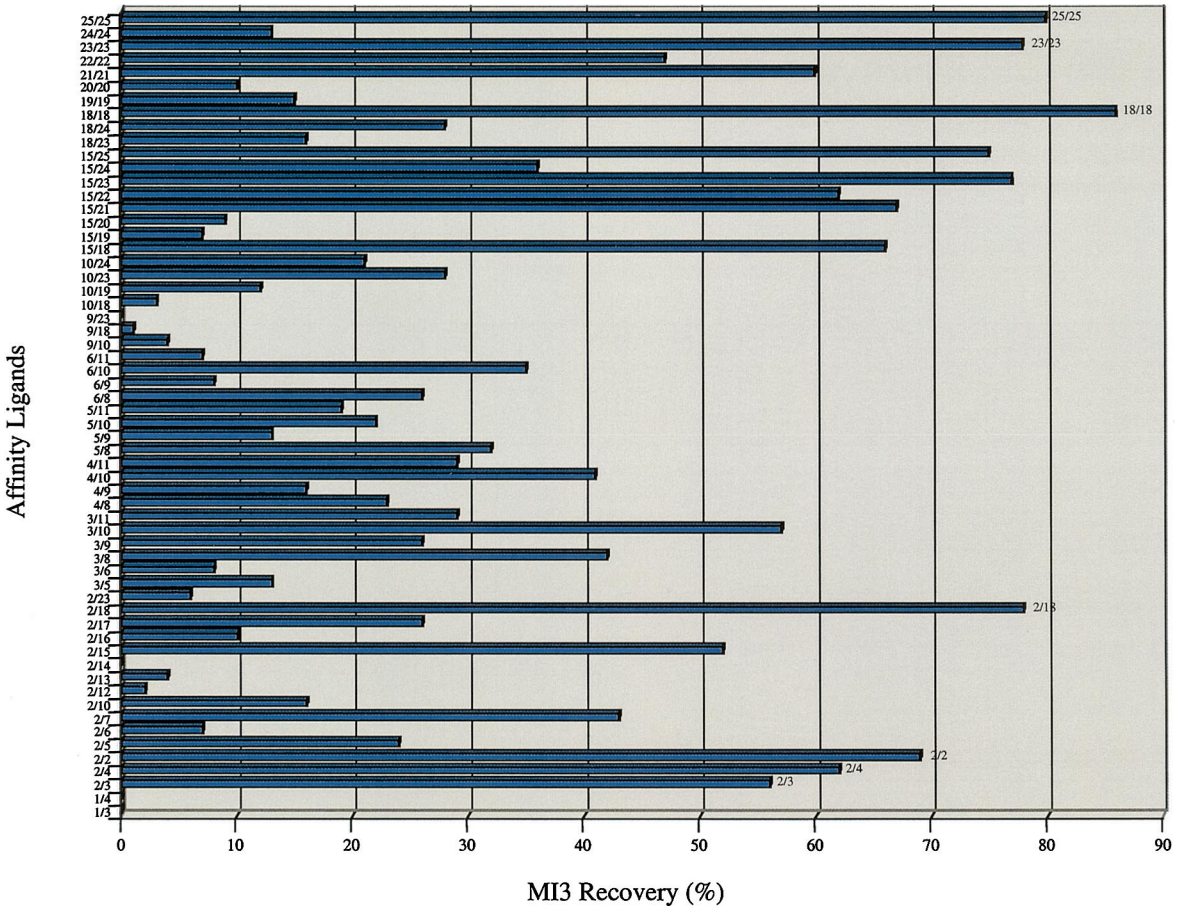

Fig. 2. Representation of the results of screening the biased combinatorial library constructed from bis-substituted triazines for recovery of purified MI3. The individual library members are designated according to numbers assigned to the amino compounds substituted in the two positions of the triazine nucleus and are tabulated along the bottom axis of the graph. Thus, ligand 1/3 comprises amino compounds 1 and 3 substituted on the triazine scaffold.

determine the overall disposition of the ligand on the matrix and thus the behaviour of the protein-immobilised ligand system. Library screening on the final matrix allows these factors to be optimised in order to achieve an effective affinity adsorbent.

3.4. Determination of quantitative binding parameters for the MI3 ligand library

Two key parameters in the identification of effective affinity ligands for the target protein are the binding constant (K_{AX}) governing the interaction between the solute (A) and the immobilised affinity ligand (X) and the total effective concentration of matrix binding sites (C''_A) [10,11]. The partition of solute between the matrix and solution states is influenced by all physico–chemical variables which affect the properties of the matrix, immobilised ligand and/or the solute. The two key quantitative parameters were determined by frontal chromatography on small columns of the immobilised ligand adsorbents using the Scatchard linear transform of the rectangular hyperbolic relationship for solute binding to a homogeneous class of matrix sites with intrinsic affinity constant K_{AX}:

$$\frac{1}{\bar{V}_A - V'_A} = \frac{1}{K_{AX} V'_A C''_X} + \frac{C'_A}{V'_A C''_X}$$

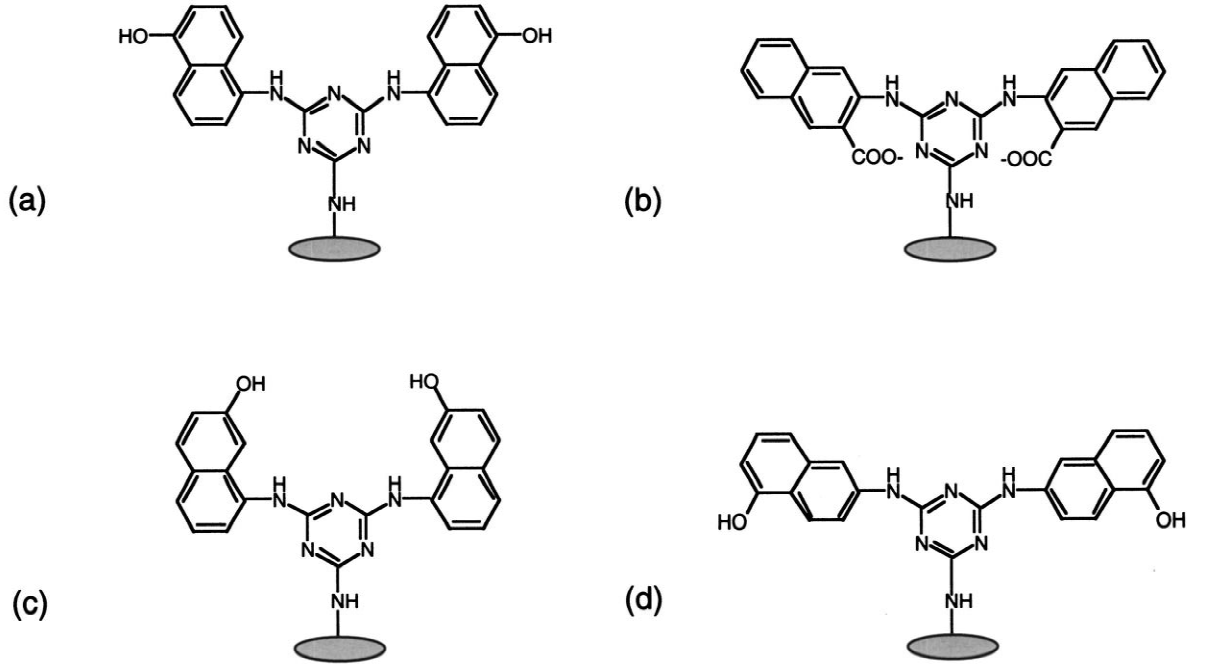

Fig. 3. The chemical structures of lead ligands for MI3 and their interaction with the protein. The structures of the symmetrical triazine ligands (a) 2/2, (b) 18/18, (c) 23/23, (d) 25/25 and (e) ligand 23/23 in yellow bound to residues B:16-Tyr and B:24-Phe in the dimer binding site of MI3.

where $\bar{V}_A$ is the elution volume of solute A determined by frontal chromatography [10,11], V'_A is the volume of the system accessible to A, i.e., the elution volume of A under conditions where no interaction of solute with the affinity adsorbent occurs, a control adsorbent, C''_X is the total effective concentration of matrix binding sites and C'_A is the total solute concentration in the mobile (solution) phase. The intrinsic association constant for the solute–matrix interaction (K_{AX}) is evaluated from the slope, whereas the concentration of matrix sites (C''_X) is inferred from the ordinate intercept.

Equilibrium association constants (K_{AX}) and binding sites concentrations (C''_X) were determined for a total of 14 adsorbents selected across the range of binding affinities for MI3 from the ligand library. Fig. 4 shows a representative breakthrough curve and Scatchard plot for immobilised ligand 2/2. The data for all the immobilised ligands is presented in Table 2 and reveals several interesting characteristics. First, despite the similarities in chemical structures of the ligands, there was an almost two-orders of magnitude difference in the association constants, within the range $8 \cdot 10^2$ M^{-1} (24/15) to $5 \cdot 10^4$ M^{-1} (42/42), for individual members of the library. Needless to say, these differences would be accentuated even further if all adsorbents in the library had been selected for study. Secondly, the calculated binding sites concentration varied within the range 48 (19/15) to 5816 μM (18/18) compared to a total ligand concentration of 15–20 μmol/g moist weight gel (15–20 mM), i.e., up to 38% of the total immobilised ligand was accessible to the MI3 protein. Thirdly, the total binding sites concentration, and hence the capacity of the adsorbent for the complementary protein, is broadly proportional ($R^2 = 0.84$) to the association constant for the protein–immobilised ligand interaction. Fourthly, asymmetric ligands synthesised on the solid phase via the two possible sequential routes often displayed differences in K_{AX} and C''_X; this feature is particularly apparent with the behaviour of the notionally identical ligands 2/18 and 18/2. It is clear that there are differences in reactivity between amines 2 (1-amino-5-naphthol)

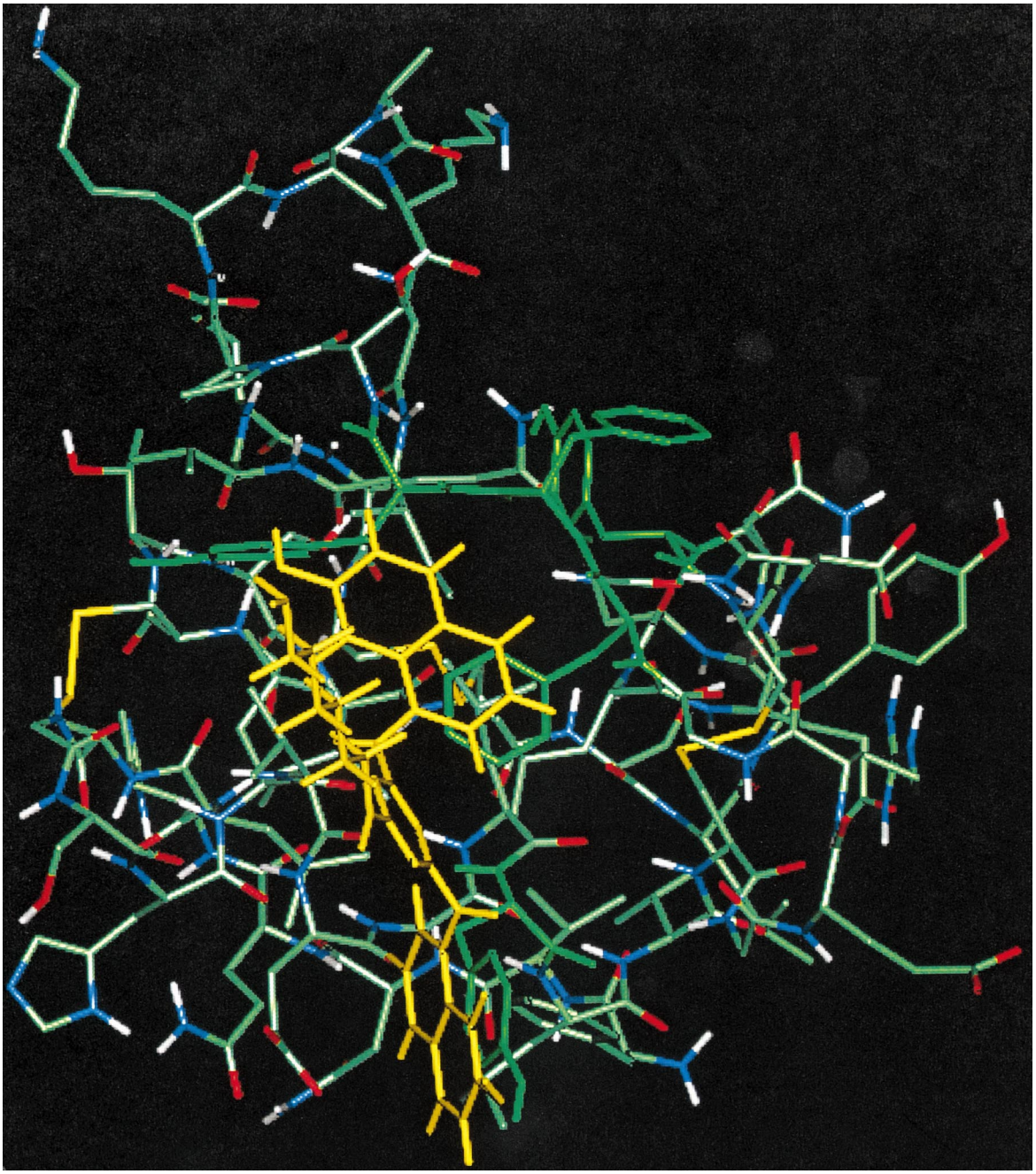

Fig. 3 (*continued*).

and 18 (3-amino-2-naphthoic acid) (Table 1) and the second and third chlorines of triazine-activated agarose which may result in differing degrees of substitution at each stage, and hence, compositions of immobilised ligands in the resulting affinity adsorbents. Finally, immobilised ligands which display

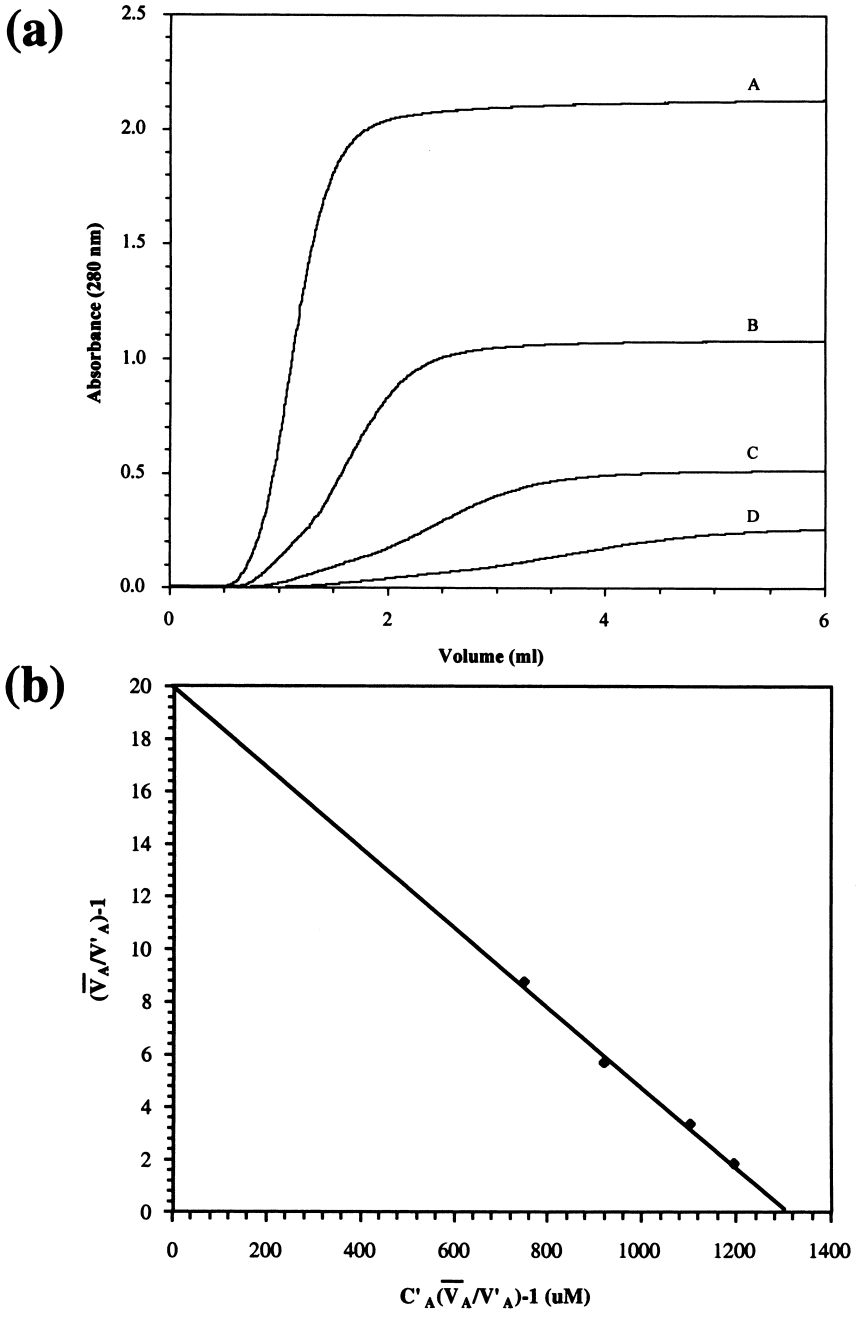

Fig. 4. The binding of the insulin anlogue MI3 to immobilised ligand 2/2 (17.5 μmol/g moist weight gel): (a) frontal analysis breakthrough curves at four concentrations of MI3 (A, 3.96 mg/ml; B, 1.99 mg/ml; C, 0.97 mg/ml; D, 0.51 mg/ml), and (b) Scatchard analysis of MI3 binding. The total binding sites concentration (C''_X) is extrapolated from the *x*-axis and the equilibrium binding constant (K_{AX}) is determined from the slope of the line.

Table 2
Binding constants (±2 SD) for the interaction of MI3 with immobilised affinity ligands

Ligand	K_{AX} ($\cdot 10^{-4}$) (M^{-1})	C''_x (μM)
42/42	4.96±0.64	3679
25/25	4.55±0.47	2908
2/18	4.13±0.36	1970
18/2	3.69±0.41	3832
23/23	2.06±0.17	2002
18/18	1.62±0.14	5807
2/2	1.51±0.16	1318
7/2	0.95±0.06	205
1/4	0.89±0.03	871
2/7	0.59±0.07	1041
15/24	0.38±0.05	218
15/19	0.33±0.04	192
19/15	0.22±0.02	48
24/15	0.08±0.008	257

high association constants ($K_{AX} > 3 \cdot 10^4\ M^{-1}$) do not necessarily result in the most effective affinity adsorbents, since the performance of the completed adsorbent depends on both the adsorption and desorption phases of the chromatography. Consequently, medium binding ligands ($K_{AX} \cong 10^4\ M^{-1}$) were selected for further optimisation.

3.5. Optimisation of the affinity adsorbent and operational parameters

The symmetrical insulin-binding ligands 2/2 (Fig. 3a) and 23/23 (Fig. 3c) were selected for further study and synthesised de novo in solution (>95% pure by TLC and reversed-phase HPLC) prior to chemical characterisation by conventional methodologies (MS and ^{1}H-NMR) and immobilisation to amino-substituted agarose beads. Preliminary data suggested that the binding of purified MI3 reached a maximum when the immobilised ligand concentration was >15 μmol/g moist weight agarose. Furthermore, and not surprisingly, in view of the small size of the target protein (M_r 5959), the extraction of MI3 from crude fermentation broth appeared to be almost independent of the nature and length of the spacer arm interposed between the ligand and the matrix backbone, with recoveries typically in the range 70–90%. Adsorbents prepared by reaction of monochlorotriazinyl-2/2 or -23/23 with the 1,6-diaminohexane derivative of epichlorohydrin-activated agarose were used in all subsequent studies.

Examination of the effect of ionic strength on MI3 binding to 2/2-agarose confirmed that 0.1 *M* NaCl added to the fermentation broth gave optimal yield of eluted protein. The column capacity was assessed by frontal analysis of breakthrough curves of purified MI3 monitored by absorbance at 280 nm and shown to be 62.8 mg purified MI3/ml gel, equivalent to 0.44 mol MI3/mol ligand 2/2 at saturation, under the adsorption conditions selected.

3.6. Purification of the insulin precursor MI3 by affinity chromatography

The elution profile at 280 nm obtained by affinity chromatography of a crude clarified and pH-adjusted (pH 5.5) yeast fermentation broth expressing the insulin precursor MI3 on a column of agarose-immobilised 23/23 is shown in Fig. 5. The concentration of MI3 in the applied sample, the flow through fraction and the eluted material was measured by reversed-phase HPLC; under the experimental conditions used the MI3 eluted in a well resolved peak with a retention time of 11.9 min (Fig. 6). The first peak in the lower panel at a retention time of 3.0 min is acetic acid used to acidify the application sample prior to analysis. Typically, the

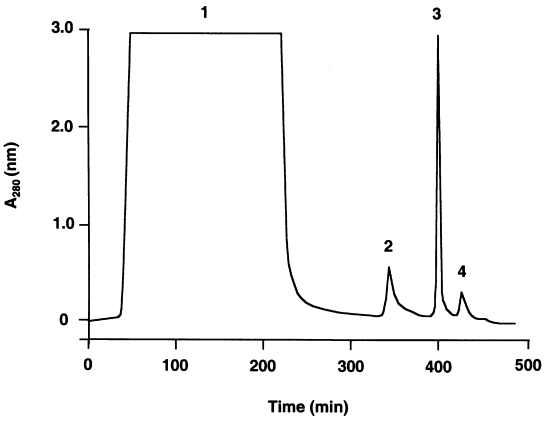

Fig. 5. Typical elution profile when a centrifuged crude yeast fermentation broth was applied to a column packed with 23/23-agarose (17.5 μmol/g moist weight gel) and showing fractions eluted in the (1) flow through, (2) MI3 eluate, (3) 0.5 *M* NaOH cleaning-in-place, and (4) 0.1 *M* citric acid–60% (v/v) ethanol cleaning-in-place.

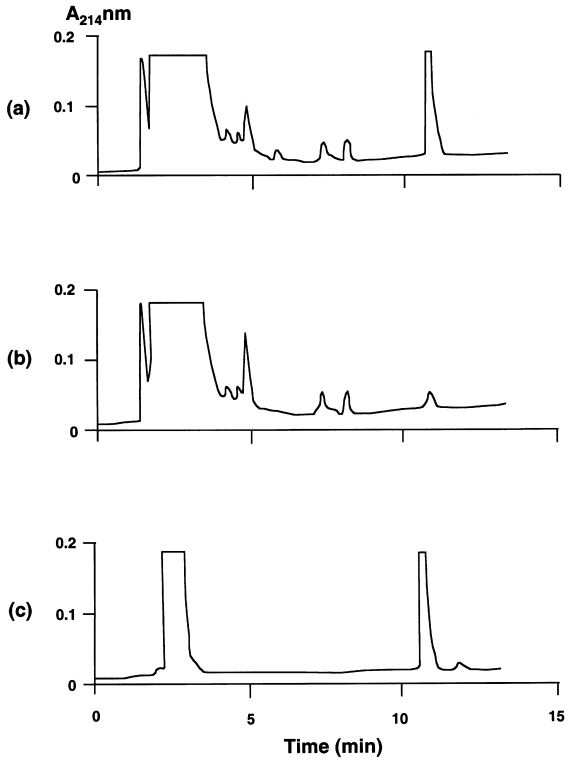

Fig. 6. Characterisation of the eluted fractions applied to the 23/23-agarose adsorbent by reversed-phase HPLC, showing the content of (a) the applied fermentation broth sample, (b) the flow through and (c) the eluted MI3.

insulin analogue MI3 was purified to yield >95% pure protein with a recovery of 90%. The dynamic binding capacity of the adsorbent determined from the breakthrough curve was estimated to be 6–7 mg MI3/g moist weight adsorbent. No visible or functional changes in the chromatographic elution profile were observed when the same column was subjected to more than 100 cycles of equilibration, adsorption, washing, elution and cleaning-in-place.

The purification procedure was followed by SDS–polyacrylaide gel electrophoresis (PAGE); it is clear from the Coomassie Blue stained gel shown in Fig. 7a that the majority of the MI3 is removed from the applied sample and eluted as a single, substantially pure, band with 0.3 *M* acetic acid. The impurity content of the eluted sample of MI3 was further assessed by overloading an SDS–PAGE gel and staining with silver (Fig. 7b): The very low content of impurities co-eluted with the MI3 were shown to be dimeric MI3 and host cell proteins (determined by Western blotting; data not shown). It was also immediately apparent on inspection of the eluted fractions that this procedure removes most of the coloured compounds associated with the initial clarified fermentation broth.

A further feature of the affinity chromatography procedure for the purification of MI3 is the possibility that the adsorbent would resolve structural isoforms of the analogue. This prospect was investigated by observing the behaviour of non-native forms of the protein obtained by reducing the two disulphide bonds in positions Cys^{A7}–Cys^{B7} and Cys^{A20}–Cys^{B19} by addition of 50 m*M* dithioerythritol to the centrifuged fermentation broth. The absence of an MI3 peak following elution from a 23/23-agarose adsorbent and confirmed by reversed-phase HPLC suggests that the affinity adsorbent may also function as an in-line quality assurance step.

3.7. The ligand binding site

Further refinements of the ligand structure to improve selectivity for the target protein or its isoforms would require identification of the site at which immobilised 23/23 binds to MI3. In practice, this is not a straightforward task, since the affinity of the immobilised ligand for MI3 is determined partly by characteristics of the ligand per se and partly by the matrix and coupling chemistry to which the ligand is immobilised. Studies in free solution with soluble ligands do not fairly reflect the chemical, geometrical and steric constraints imposed by the complex three-dimensional matrix environment. However, exploratory studies on the interaction of free monochlorotriazinyl ligand 23/23 with MI3 by high-resolution 600 MHz NMR spectroscopy were conducted, but proved unsuccessful. Free ligand 23/23 displays limited solubility in aqueous or polar media and the identification of a suitable solvent for both the ligand and MI3 proved elusive. The ligand appears to exhibit a relatively low intrinsic affinity for MI3 in free solution and would require a concentration well above its solubility to alter the protein NMR spectrum. Furthermore, even if suitable solvent conditions could be found and perturbations in the NMR spectrum observed, it is doubtful if any

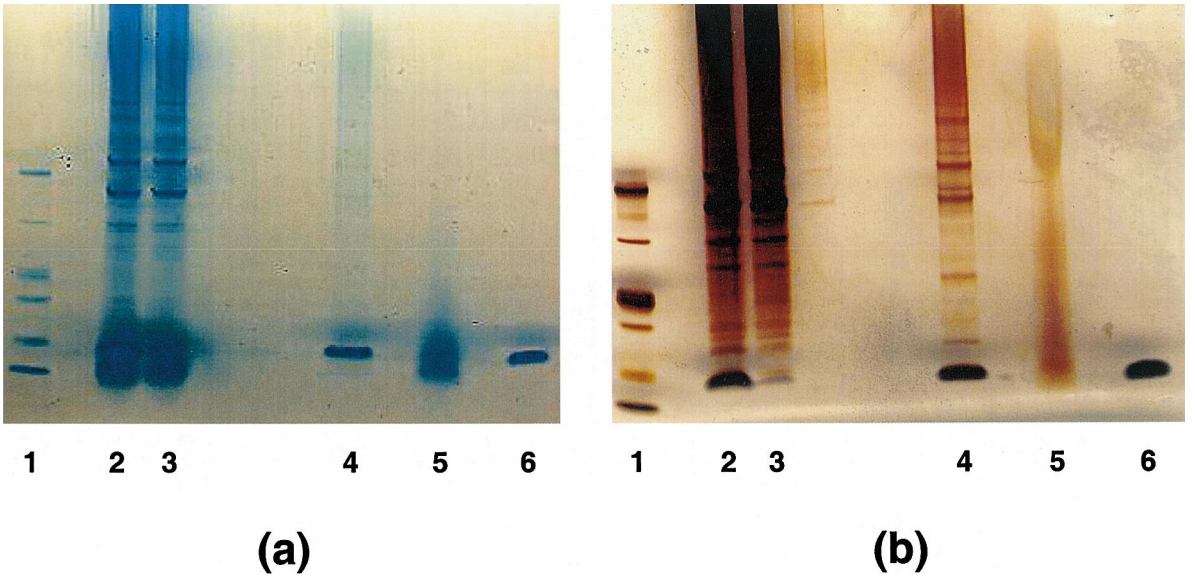

Fig. 7. SDS–PAGE analysis of the fractions eluted from the 23/23-agarose affinity adsorbent and stained with Coomassie Blue (a) and silver (b), showing: lane 1, molecular mass markers; 2, applied sample; 3, flow through; 4, MI3 eluate; 5, 0.5 *M* NaOH cleaning-in-place; 6, authentic MI3 standard.

conclusions drawn from interactions in solution, would be valid for the immobilised ligand system.

4. Implications of the work

The design strategy implemented in this report comprises four distinct stages; (i) modelling of the target site and design of a complementary ligand, (ii) limited solid-phase synthesis of a combinatorial library of near-neighbour compounds, (iii) solution phase synthesis and characterisation of lead ligands, and (iv) immobilisation, optimisation and final chromatography of the target protein. The dependence on a defined structural template which formed the basis for earlier strategies [7,8] has been obviated by the synthesis of a limited combinatorial library of ligands and the use of parallel screening for target protein binding and elution. The power of this strategy for obtaining selective affinity ligands is further established by the ease in which defined chromatographic conditions can be incorporated into the screening conditions from the outset.

The use of a synthetic biomimetic ligand offers several advantages for the purification of biopharmaceuticals: In particular, the adsorbents are inexpensive, scaleable, durable, readily reusable over multiple cycles and provide a ligand of defined chemistry and toxicity to satisfy the regulatory authorities. Preliminary studies on the ligands reported here has shown that neither the ligands per se nor the potential column leachates are toxic. Furthermore, the stability of synthetic matrices to harsh elution and cleaning-in-place protocols exceeds antibodies and removes the potential risk of prion or viral contamination from animal sources [18,19]. Similarly, oligopeptide ligands derived from domains of larger proteins such as Staphylococcal protein A, which have been shown to purify insulin [20], would still prove less durable under harsh sterilisation and cleaning conditions.

The ligands reported in this paper display a high degree of selectivity for the insulin analogue MI3, with the movement of a single hydroxylic substituent on the naphthalene nucleus from the 5 to the 4 position converting a very effective adsorbent into a non-binder. It is not clear, however, whether the ligands bind at the targeted binding site on the dimer interface or how this selectivity is achieved, although $\pi-\pi$, hydrophobic and hydrogen bonding interac-

tions are likely to be implicated. Attempts to resolve these issues to date have proven inconclusive.

Acknowledgements

The authors would like to thank Nicola Blair formerly of ProMetic BioSciences Inc. and Marianne Guldmann and Jette Lundgren from Novo Nordisk A/S for excellent technical assistance, Niels C. Kaarsholm for his help in identifying the binding site from the MI3 structure, Svend Havelund for supplying the human insulin mutants, Ane Blom for assisting with the sample preparation for the NMR and Guy Dodson and Jean Whittingham, Department of Chemistry, University of York for providing information on the protein folding of MI3.

References

[1] C.R. Lowe, S.J. Burton, N.P. Burton, W.K. Alderton, J.M. Pitts, J.A. Thomas, Trends Biotechnol. 10 (1992) 442–448.
[2] E. Harlow, D. Lane, Antibodies – A Laboratory Manual, Cold Spring Harbor Laboratory Press, Cold Spring Harbor, NY, 1988, pp. 511–552.
[3] K.T. O'Neil, F. DeGrado, R.H. Hoess, Techniques in Protein Chemistry, Vol. V, Academic Press, 1994, pp. 517–524.
[4] A. Murray, J. Sekowski, D.I.R. Spencer, G. Denton, M.R. Price, J. Chromatogr. A 782 (1997) 49–54.
[5] C.R. Lowe, S.J. Burton, J.C. Pearson, S.B. McLoughlin, N.P. Burton, S. Dilmaghanian, Y.D. Clonis, C.V. Stead, Biol. Chem. Hoppe-Seyler 368 (1987) 759–760.
[6] S.B. McLoughlin, C.R. Lowe, Rev. Prog. Coloration 18 (1988) 16–28.
[7] N.P. Burton, C.R. Lowe, J. Mol. Recognit. 6 (1993) 31–40.
[8] R.-X. Li, V. Dowd, D.J. Stewart, S.J. Burton, C.R. Lowe, Nature Biotechnol. 16 (1998) 190–195.
[9] P.M. Doyle, J. Chem. Technol. Biotechnol. 64 (1995) 317–324.
[10] D.J. Winzor, C.M. Jackson, in: T. Kline (Ed.), Handbook of Affinity Chromatography, Marcel Dekker, New York, 1993, pp. 253–298.
[11] D.J. Winzor, in: P. Matejtschuk (Ed.), Affinity Separations – A Practical Approach, IRL Press, Oxford, 1997, pp. 39–60.
[12] M.J. Adams, T.L. Blundell, E.L. Dodson, G.G. Dodson, M. Vijayan, E.N. Baker, M.M. Harding, D.C. Hodgkin, R. Rimmer, S. Sheet, Nature 224 (1969) 491–496.
[13] T.L. Blundell, J.F. Cutfield, S.M. Cutfield, E.J. Dodson, G.G. Dodson, D.C. Hodgkin, D.A. Mercola, Diabetes 21 (1972) 492–499.
[14] S. Ludvigsen, M. Roy, H. Thøgersen, N.C. Kaarsholm, Biochemistry 33 (1994) 7998–8006.
[15] G.G. Dodson, J. Whittingham, personal communication.
[16] J.T. Thurston, J.R. Dudley, D.W. Kaiser, I. Hechenbleikner, F.C. Schaefer, D. Holm-Hansen, J. Am. Chem. Soc. 73 (1951) 2981–2983.
[17] H. Neunhoeffer, Chemistry of 1,2,3-Triazines, 1,2,4-Triazines, Tetrazines and Pentazines, Wiley, New York, 1978.
[18] G.W. Jack, H.E. Wade, TIBTECH 5 (1987) 91–95.
[19] A. Jungbauer, E. Boschetti, J. Chromatogr. B 662 (1994) 143–179.
[20] K. Nord, E. Gunneriusson, J. Ringdahl, S. Ståhl, M. Uhlén, P.Å. Nygren, Nature Biotechnol. 15 (1997) 772–777.